Supporting Information

Hydrogen Spillover on Rh/TiO_2: FTIR Study of Donated Electrons, Coadsorbed CO and H/D Exchange

D. Panayotov,[1*] E. Ivanova,[2] M. Mihaylov,[2] K. Chakarova,[2] T. Spassov,[1] and K. Hadjiivanov[2*]

[1] *University of Sofia, Department of Chemistry and Pharmacy, Sofia 1126, Bulgaria*

[2] *Institute of General and Inorganic Chemistry, Bulgarian Academy of Sciences, Sofia 1113, Bulgaria*

(*) corresponding authors: dapanayotov@hotmail.com , kih@svr.igic.bas.bg

SI A. Characterization of Rh/TiO_2 samples. Background spectra

Activated TiO_2 and Rh/TiO_2 samples

The transmission IR spectrum of as activated reference TiO_2 sample (Figure S1, spectrum *a*) exhibits a limited amount of isolated surface Ti–OH groups. The bands appearing at 3719, 3690 and 3670 cm^{-1} (spectrum *a* in the inset of Figure S1) well agree with previously reported spectra of activated TiO_2.[1-3] The absence of bands in the regions of δ(HOH) modes (~ 1630 cm^{-1}) and H-bonded hydroxyls (3600 – 3000 cm^{-1}) indicates that the activated TiO_2 sample was highly dehydroxylated.

The FTIR transmission spectrum of 1.3 wt.% Rh/TiO_2 sample (Figure S1, spectrum *b*) shows a progressively increasing background absorbance for wavenumbers higher than 1800 cm^{-1}. We attribute this spectral change (as compared to pure TiO_2 sample) to the presence of deposited Rh nanoparticles that cause wavenumber-dependent dispersion of IR photons. The IR spectrum in the region of ν(OH) vibrations (spectrum *b* in the inset of Figure S1) is close to that of the reference TiO_2 sample. These results suggest that loading of Rh nanoparticles onto TiO_2 hardly affect the hydroxyl coverage of the TiO_2 support.

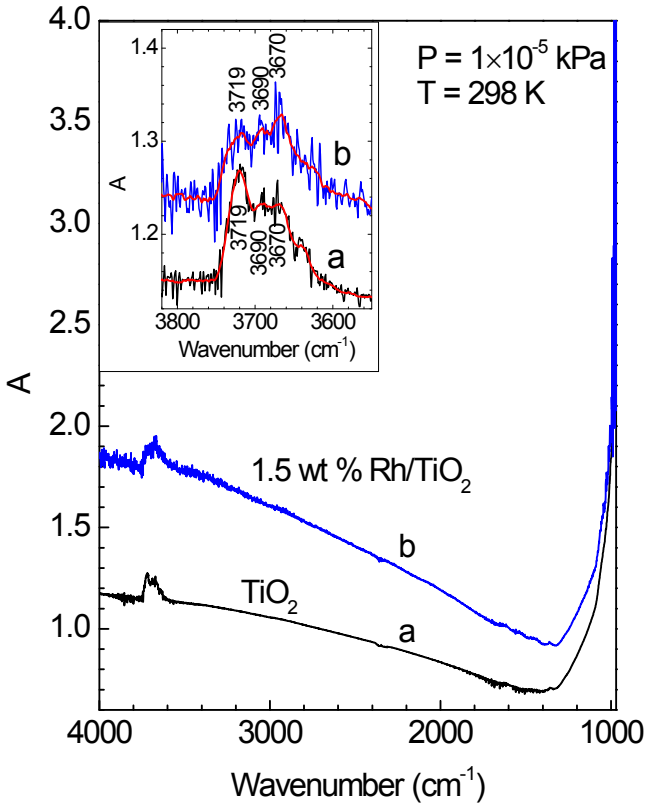

Figure S1. Transmission FTIR spectra of as activated TiO_2 and Rh/TiO_2 samples; The inset: spectra in the region of isolated surface Ti–OH groups.

H_2-reduced Rh/TiO_2 sample

The IR spectrum of the H_2-reduced Rh/TiO_2, registered in presence of gaseous H_2 (Figure S2 A, spectrum *b*) is characterized by an enormous IR background absorbance observed throughout the whole 4000 – 1000 cm^{-1} range. This strong featureless mid-IR absorbance was attributed to free and shallow trapped electrons in TiO_2, as previously reported for TiO_2 reduced via high temperature treatment (923 K) *in vacuo*.[2,4] In both cases, extra electrons are accumulated in TiO_2 due to lattice oxygen extraction via interaction with H_2 or thermal activation, respectively, (see the next section for more details). Subsequent evacuation of Rh/TiO_2 sample at 523 K (spectrum *c* in Figure S2 A) resulted in a substantial decrease in the IR background absorbance due to depletion of charges via recombination or deep trapping.[2]

However, the initial background absorbance (spectrum *a* in Figure S2 A) was fully restored only after addition of molecular oxygen (spectrum not shown). Oxygen has strong affinity to electrons and when adsorbed (even at room temperature) it depletes the residual free and ST electrons from the TiO_2.[5] These observations evidence the electronic character of

observed profound increase in the IR background absorbance of reduced TiO_2. The spectrum of H_2-reduced sample also showed a slight increase in the intensity of bands attributed to surface OH groups and adsorbed water.

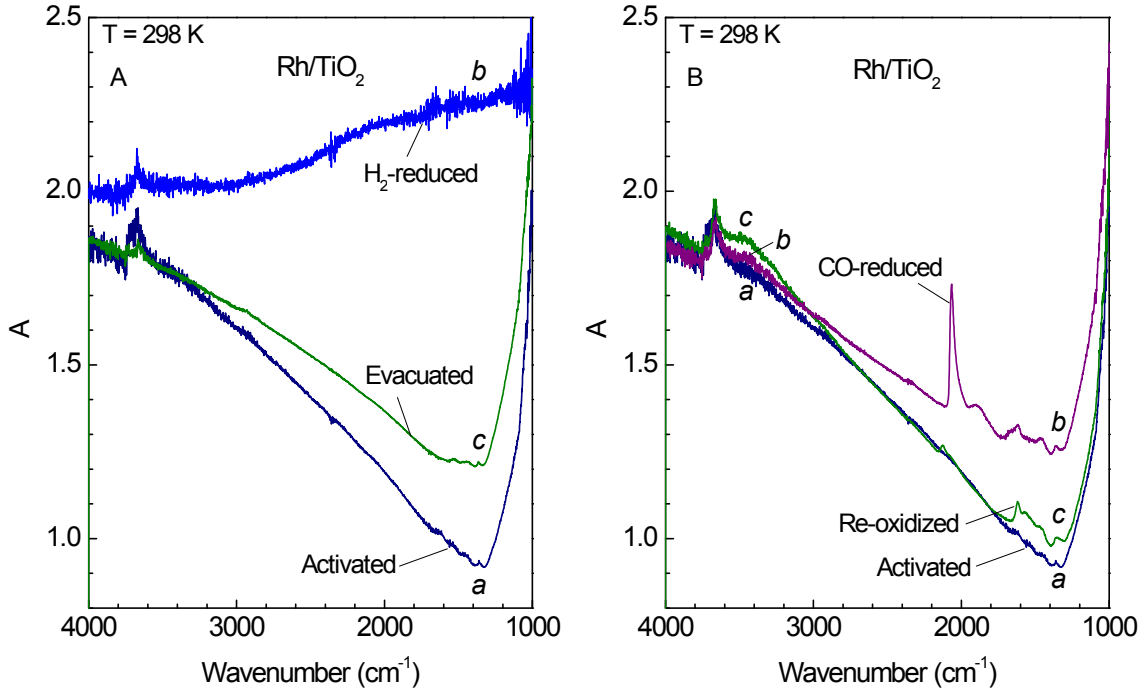

Figure S2. Transmission FTIR spectra of Rh/TiO_2 samples obtained after activation, H_2 and CO reduction and partial re-oxidation in O_2. See the experimental section for detailed description of these treatments. Panel A: spectra of (a) activated, (b) H_2-reduced and (c) evacuated (following b) Rh/TiO_2 samples. Panel B: spectra of (a) activated, (b) CO-reduced and (c) re-oxidized (following b) Rh/TiO_2 samples.

CO-reduced Rh/TiO₂ sample

Reduction of activated Rh/TiO_2 sample with CO gas at 523 K caused analogous but much lower increase in the IR background absorbance (Figure S2 B, spectrum *b*) as compared to that obtained via H_2 reduction (Figure S2 A, spectrum *b*). This indicated that (i) the reduction process is mainly associated with the supported Rh phase and (ii) the reduction of the TiO_2 support is limited in absence of hydrogen. Other consequences of CO reduction were the appearance of (i) strong bands at 2065 and 1900 cm^{-1} belonging to linear Rh^0–CO and bridged Rh_x^0-CO species, respectively, formed on the surface of reduced Rh crystallites;[6] and (ii) bands in the 1560 – 1360 cm^{-1} spectral region that were associated with carbonate structures formed on the TiO_2 support.[7-10]

Re-oxidized Rh/TiO_2 sample

Exposure of CO-reduced Rh/TiO_2 sample to 3 kPa molecular O_2 at 298 K returned immediately the background absorbance to the level of activated sample, as revealed by the comparison of spectra *c* and *a* in Figure S2 B. In this case, the carbonate bands gained some intensity.

SI B. Characterization of Rh/TiO_2 samples. Spectra of adsorbed CO

Figure S3 summarizes the spectra in the carbonyl-stretching region obtained with differently pre-treated samples after exposure to gas-phase CO and evacuation.

Activated Rh/TiO_2 and TiO_2 samples

The IR spectra of both activated Rh/TiO_2 and TiO_2 samples obtained immediately after introduction of 4 kPa CO (spectra *a* and *a'*, respectively, in Figure S3 A) showed a band at 2186 cm^{-1} indicating the formation of carbonyls linearly bound at coordinatively unsaturated Ti sites ($Ti^{4+}_{(CUS)}$) on TiO_2 surface.

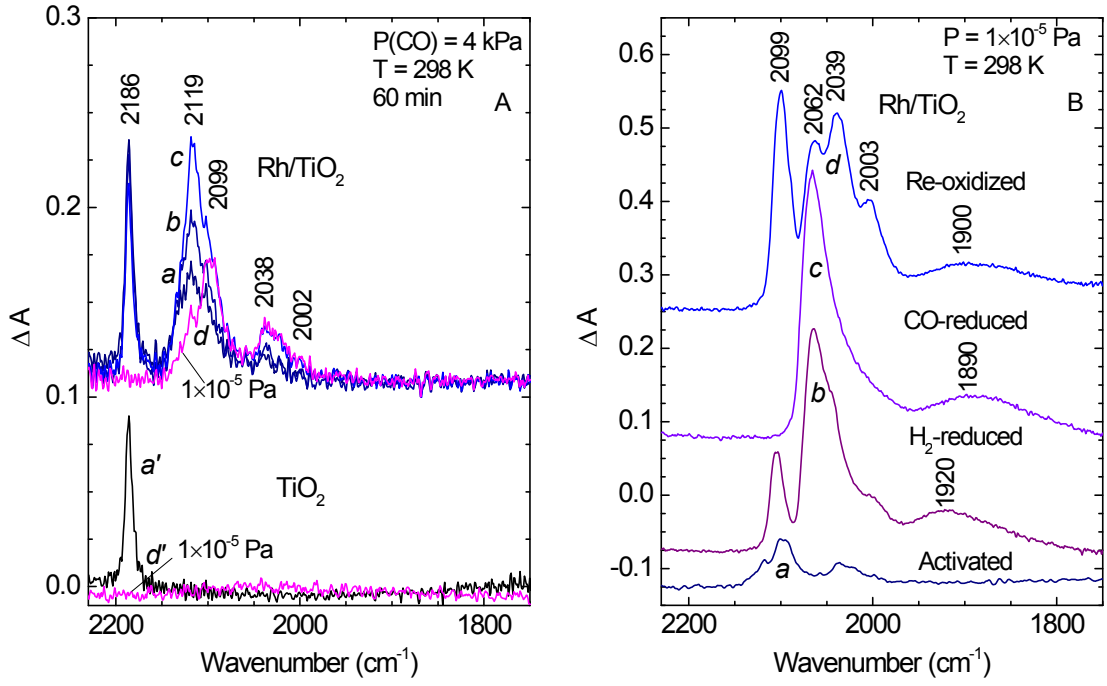

Figure S3. Difference IR spectra of CO probe molecule adsorbed on: (A) activated TiO_2 and Rh/TiO_2 samples; (B) Reduced and re-oxidized Rh/TiO_2 samples. The samples were first saturated with CO and then evacuated at 298 K to P = 1 × 10–5 Pa.

These carbonyl species were unstable and disappeared under evacuation at room temperature (spectra *d* and *d'*). Carbon monoxide weakly bound to ionic Rh^{n+} (n = 2 or 3) sites on oxidized rhodium crystallites was detected at 2119 cm^{-1}.[11,12] The intensity of this band slowly increased with the time of CO exposure (spectra *a–c* in Figure S3 A) indicating that oxidized Rh^{n+} sites were not accessible for CO adsorption on the activated Rh/TiO_2. The doublet appearing at 2099 and 2038 cm^{-1} was assigned to symmetric and antisymmetric vibrations of isolated geminal dicarbonyls, $Rh^{I}(CO)_2$.[13-16] The linear (or mono) carbonyls of Rh^{n+} were unstable and their concentration decreased upon decreasing the equilibrium pressure of CO and evacuation. As expected,[13-16] the $Rh^{I}(CO)_2$ species resisted evacuation (spectrum *d*). Their characteristic bands even slightly increased in intensity suggesting reduction of some Rh^{n+} species to Rh^{+} during the experiments. Thus, the activated Rh/TiO_2 sample exhibited cationic, but no metallic rhodium sites. The overall intensity of the carbonyl bands with this sample pre-treatment is weak which suggests that some Rh^{n+} sites are coordinatively saturated and are thus not able to coordinate CO.

H_2-reduced Rh/TiO_2 sample

The spectrum of CO adsorbed on H_2-reduced Rh/TiO_2 sample that was pre-evacuated at 298 K (Figure S3 B, spectrum *b*) showed an intense band at 2064 cm^{-1} unambiguously assigned to linear Rh^0–CO species and a broad band at 1920 cm^{-1} characteristic of bridged Rh_x^0-CO carbonyls.[16,17,18] In addition, a band at 2099 cm^{-1} was registered and attributed to the symmetric modes of isolated $Rh^{I}(CO)_2$ geminal species,[14,16,17,19] the respective antisymmetric modes (the shoulder at ~2040 cm^{-1}) are masked by the intense band of Rh^0–CO. These data indicated that the metallic Rh particles obtained through H_2-reduction were easily disrupted upon CO adsorption to give isolated Rh(I) geminal dicarbonyls, as widely discussed in the literature.[14,16,17]

CO-reduced Rh/TiO_2 sample

The CO-reduced Rh/TiO_2 sample was first saturated with CO (4 kPa CO at 298 K, for 120 min). After evacuation at 298 K, the sample was almost fully covered with CO, i.e. θ_{CO} = 0.9, as shown in Figure S3 B, spectrum *c*. The spectrum confirmed the presence of only metallic Rh^0 sites. The band at 2065 cm^{-1} is due to linear Rh^0-CO species, while the wide band centered at 1890 cm^{-1} is attributed to bridged Rh_2^0CO species, as previously reported.[6,16,17] No geminal dicarbonyl species bound to isolated Rh cations were detected for this CO-reduced Rh/TiO_2, which indicates that rhodium particles on the sample were highly

resistant to the corrosive action of CO. This implies formation of metallic Rh nanoparticles with low concentration of defect sites.[6]

Re-oxidized Rh/TiO_2 sample

Re-oxidation of CO–reduced Rh/TiO_2 sample with O_2 strongly promoted the formation of isolated $Rh^I(CO)_2$ geminal species after subsequent CO adsorption (Figure S3 B, spectrum *d*). The pair of bands at 2099 and 2039 cm^{-1} is due to isolated $Rh^I(CO)_2$ species.[14-19] The bands appearing at 2062 and 1900 cm^{-1} are attributed to linear Rh^0CO and bridging Rh^0_xCO species, respectively, formed on metallic Rh^0 sites.[14-19] An estimate based on the integrated absorbance of linear carbonyls showed that about 50% of metallic Rh was converted into oxidized Rh species. Therefore, a substantial part of Rh sites adsorbing CO remained in metallic Rh^0-state on this re-oxidized Rh/TiO_2 sample. The band at 2003 cm^{-1} was more difficult to assign. Guglielminotti and Boccuzzi[20] attributed a similar band to Rh^+(Cl)-CO species. Our data do not support this assignment because the band was detected only with the re-oxidized sample. A carbonyl band at 2017 cm^{-1} was assigned to Rh^+-(CO)-Rh^+ species.[21] Note that gem dicarbonyls are observed at 2075 and 2000 cm^{-1} with Rh/MgO[22] and at 2109 and 2000 cm^{-1} with Rh/X zeolite.[23] Therefore, it seems that the 2003 cm^{-1} band is due to geminal dicarbonyls that are not isolated on the support, but probably formed on Rh^+ sites at the periphery of metal particles.

SI C. TEM and HRTEM images of Rh/TiO_2 sample

TEM study of ex-situ CO-reduced Rh/TiO_2 sample (Figure S4 A) revealed decoration of TiO_2 particles (average size 25 nm) by pseudo-hemispherical Rh nanoparticles that have a narrow distribution of particles sizes with mean diameter $d_p \approx 2.2$ nm.[6] HRTEM study of Rh/TiO_2 sample showed (Figure S4 B and C) that Rh nanoparticles with different exposed faces are preferentially grown on different TiO_2 crystal planes. Lattice fringes (101) of anatase TiO_2 coexisted with (111) lattice fringes of rhodium while lattice fringes (100) of anatase coexisted with (100) lattice fringes of rhodium.

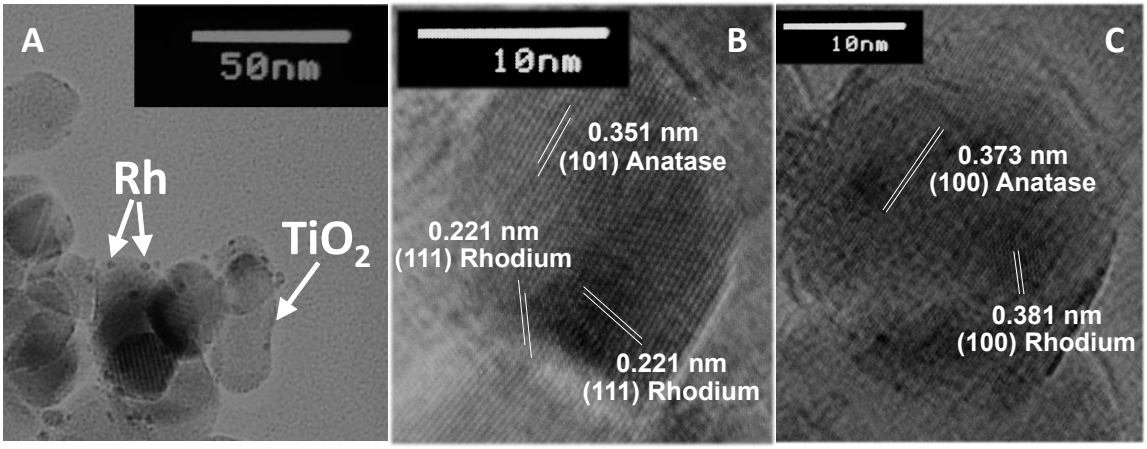

Figure S4. (A) Bright field TEM image of the 1.3 wt. % Rh/TiO_2 sample. (B) and (C) HRTEM images of ~ 25 nm anatase particles bearing ~ 2–3 nm Rh particles.

References

(1) Szczepankiewicz, S. H.; Moss, J. A.; Hoffmann, M. R. *J. Phys. Chem. B* **2002**, *106*, 7654.
(2) Panayotov, D. A.; Yates Jr, J. T. *Chem. Phys. Lett.* **2005**, *410*, 11.
(3) Panayotov, D. A.; Morris, J. R. *J. Phys. Chem. C* **2009**, *113*, 15684.
(4) Panayotov, D. A.; Burrows, S. P.; Morris, J. R. *J. Phys. Chem. C* **2012**, *116*, 4535.
(5) Berger, T.; Sterrer, M.; Diwald, O.; Knözinger, E.; Panayotov, D.; Thompson, T. L.; Yates Jr, J. T. *J. Phys. Chem. B* **2005**, *109*, 6061.
(6) Panayotov, D.; Mihaylov, M.; Nihtianova, D.; Spassov, T.; Hadjiivanov, K. *PCCP* **2014**, *16*, 13136.
(7) Hadjiivanov, K. *Appl. Surf. Sci.* **1998**, *135*, 331.
(8) Binet, C.; Daturi, M.; Lavalley, J.-C. *Catal. Today* **1999**, *50*, 207.
(9) Martra, G. *Appl. Catal. A* **2000**, *200*, 275.
(10) Venkov, T.; Fajerwerg, K.; Delannoy, L.; Klimev, H.; Hadjiivanov, K.; Louis, C. *Appl. Catal. A* **2006**, *301*, 106.
(11) Wey, J. P.; Neely, W. C.; Worley, S. D. *J. Catal.* **1992**, *134*, 378.
(12) Frank, M.; Kühnemuth, R.; Bäumer, M.; Freund, H. J. *Surf. Sci.* **1999**, *427–428*, 288.
(13) Yates, J. J. T.; Duncan, T. M.; Worley, S. D.; Vaughan, R. W. *J. Chem. Phys.* **1979**, *70*, 1219.
(14) Basu, P.; Panayotov, D.; Yates, J. T. *J. Am. Chem. Soc.* **1988**, *110*, 2074.
(15) Solymosi, F.; Knozinger, H. *J. Chem. Soc., Faraday Trans.* **1990**, *86*, 389.
(16) Zhang, Z. L.; Kladi, A.; Verykios, X. E. *J. Mol. Catal.* **1994**, *89*, 229.
(17) Buchanan, D. A.; Hernandez, M. E.; Solymosi, F.; White, J. M. *J. Catal.* **1990**, *125*, 456.
(18) Sean, M. M.; Lundwall, M.; Yang, F.; Zhou, Z.; Goodman, D. W. *J. Phys.: Condens. Matter* **2009**, *21*, 474223.
(19) Solymosi, F.; Pasztor, M. *J. Phys. Chem.* **1986**, *90*, 5312.
(20) Guglielminotti, E.; Boccuzzi, F. *J. Mol. Catal. A: Chem.* **1996**, *104*, 273.
(21) Trautmann, S.; Baerns, M. *J. Catal.* **1994**, *150*, 335.

(22) Gutschick, D.; Miessner, H. *React. Kinet. Catal. Lett.* **1984**, *26*, 387.
(23) Yamanis, J.; Yang, K.-C. *J. Catal.* **1981**, *69*, 498.